

Quasi-gaussian velocity distribution of a vibrated granular bilayer system

ALEXIS BURDEAU and PASCAL VIOT

Laboratoire de Physique Théorique de la Matière Condensée, Université Pierre et Marie Curie, 4, place Jussieu, 75252 Paris Cedex 05, France

PACS 45.70.Qj –

PACS 89.75.Kd –

Abstract. - We show by using a Discrete Element Method that a bilayer of vibrated granular bidisperse spheres exhibits the striking feature that the horizontal velocity distribution of the top layer particles has a quasi-Gaussian shape, whereas that of the bottom layer is far from Gaussian. We examine in detail the relevance of all physical parameters (acceleration of the bottom plate, mass ratio, layer coverage). Moreover, a microscopic analysis of the trajectories and the collision statistics reveal how the mechanism of randomization.

Granular particle dynamics and granular flows are dominated by dissipation due to the inelastic collisions occurring between particles. In the last twenty years, many studies have been carried out on these non-equilibrium systems, revealing several specific features. Many of the experimental studies have focused on vibrated granular media [1]. Among these systems vibrated granular layers are of particular interest: a large variety of patterns occur [2], for example two-phase coexistence [3], clustering [4] or melting [5]. At high density, monolayer systems display many behaviors observed in glassformers such as a stretched intermediate scattering function [6, 7] and dynamic heterogeneities [6]. The way energy is injected into these systems is of crucial importance for their thermodynamic properties.

The theoretical treatment of energy injection in granular systems remains an open problem. In the framework of kinetic theory, used for dilute granular flows, several “thermostats” have been formally introduced to inject energy to the granular particles. They consist of applying external forces to each particle of the system. The velocity distributions obtained in these cases are dependent on the way energy is supplied. Two types of thermostats have been extensively studied; the so-called Stochastic thermostat [8] where the force is a white noise, and the Gaussian thermostat [9] where the force is a Langevin-like force. These two models both lead to nearly Gaussian velocity distributions. Another trick commonly used to inject energy in kinetic theory is to consider a tracer in a Gaussian bath. The

tracer undergoes inelastic collisions with the bath particles, whereas the latter collide elastically with each other. The velocity distribution obtained for the tracer in this case is purely Gaussian [10, 11]. Up to now, these theoretical cases have not been explicitly related to experimental situations.

Recent experiments clarifying the mechanism of energy injection in quasi-2D vibrated systems have been reported. They revealed that non-equilibrium steady states (NESS) can display features surprisingly close to those observed in equilibrium systems: Prevost *et al.* [12] investigated a monolayer of steel beads on a base plate subject to a sinusoidal displacement. When the plate is rough and the density is low, the velocity distribution is very similar to a Gaussian. In their recent work, Reis *et al.* [13] have claimed to observe characteristic features of the stochastic thermostat on the velocity distribution of a vibrated granular monolayer. Baxter and Olafsen [14] have experimentally studied a vibrated bilayer system, where the bottom layer was dense and composed of steel beads and the top layer was composed of plastic beads. The base of the cell, a horizontal circular plate, was vibrated sinusoidally in the vertical direction. In these experiments, the excitation was tuned via the dimensionless acceleration defined as $\Gamma = A(2\pi f)^2/g$, where g denotes the gravity, A the amplitude of the oscillations and f the frequency. The values of Γ used varied from 1.75 to 2.25 such that the layers were stable. The coverage density of the top layer, defined as the ratio of the number of particles in the layer

divided by the number of particles there would be in a closed packed configuration, was varied from $c = 0.2$ to $c = 0.8$. The horizontal velocities of light particles (second layer) were monitored to build the velocity distribution function. Deviations from Gaussian are quantified by the kurtosis $F = \frac{\langle v^4 \rangle}{\langle v^2 \rangle^2}$, which is equal to 3 for a Gaussian distribution. The experimental results showed that the horizontal velocity distributions of the top layer were very close to Gaussian, ($|F - 3| \leq 0.05$), within the parameters range presented above (acceleration, density, particle size). Conversely, the horizontal velocity distribution of the heavy-particle layer, as well as the vertical velocity distributions remained strongly non Gaussian ($|F - 3| \geq 1$).

The purpose of this paper is twofold: first to build a simple, but realistic model which captures the observed features; second, to analyze microscopic quantities to obtain insight into the role of the first layer and the mechanisms responsible for this apparent equilibrium behavior. In order to examine the robustness of this behavior, we investigated the dependence of the kinetic properties on the mass of the top-layer particles. We also considered the situation where the particles of the first-layer are glued to the vibrating plate, in order to measure separately the role of the roughness of the first layer and that of the temperature of the first-layer particles.

Our simulation model consists of a number N_1 of heavy spherical particles placed at the bottom of the simulation cell and N_2 light spherical particles forming the second layer. Periodic boundary conditions are used in horizontal directions. We checked that the role of the boundary conditions is negligible for the properties of the steady state by varying the size of the simulation cell. In this study, the simulations were carried out on a system with 2500 spheres in the first layer. Initially, these spheres are placed on a triangular lattice, with the packing fraction of the first layer equal to $\eta = 0.9$ (or $c = 1$).

The bottom plate follows a sinusoidal displacement with frequencies ranging from 50Hz to 90Hz . Keeping the dimensionless acceleration constant $\Gamma = 2$, namely decreasing the bottom plate vibration amplitude A , we do not observe variations of the kurtosis F in this frequency range. In addition, we also increased the acceleration Γ but for $\Gamma > 2.5$ we observed a rapid irreversible mixing between the two layers which definitely corrupts the setup.

The collisions between spheres, as well as the collisions between spheres and the vibrating bottom, are inelastic. In addition to collisions, the particles are subject to a constant acceleration due to the (vertical) gravitational field. The visco-elastic forces are modeled by the spring-dashpot model [15].

Let us consider two spheres labeled 1 and 2. The respective virtual overlap ξ between the two particles is given by

$$\xi = \max(0, (R_1 + R_2 - |\mathbf{r}_1 - \mathbf{r}_2|)). \quad (1)$$

Let \mathbf{n} be the unit vector pointing from the center of particle 1 to the center of particle 2. The simplest force along \mathbf{n}

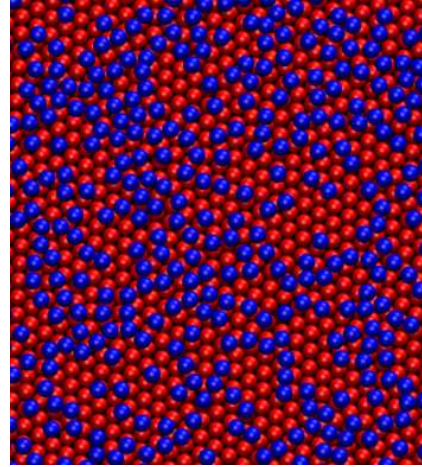


Fig. 1: Snapshot of a 50×50 system used in our simulations. The bottom particles (red) are densely packed on a quasi-perfect triangular lattice. The coverage of light particles (blue) is $c = 0.4$.

that takes dissipation into account is a damped harmonic oscillator force defined as :

$$F_n = -k_n \xi - \gamma_n \dot{\xi} \quad (2)$$

where k_n is related to the stiffness of the material, and γ_n to the dissipation. This force model allows one to very easily tune certain quantities in the simulation, especially the normal coefficient of restitution e_n , which is constant for all collisions at all velocities in our system. Relevant values of e_n and t_n determine the values of k_n and γ_n , independently of the velocities. The choice of the collision duration t_n , naturally introduces a microscopic characteristic time. For the Verlet algorithm using a constant time step, we have verified that $\Delta t = t_n/100$ is a good choice for accurate results.

In addition, we introduce a frictional force by taking the tangential component of the force as follows:

$$F_t = -\min(|k_t \zeta|, |\mu F_n|) \quad (3)$$

where k_t is related to the tangential elasticity and ζ is the tangential displacement since the contact was first established. As k_t is related to the stiffness of the material, its value depends on that of k_n (we used a ratio $k_t/k_n = 2/7$ in our simulations).

In their experiments, Olafsen and Baxter [14] used flexible dumbbells in place of spheres in the first layer. For the sake of simplicity, we have used simple spheres. Since the density of the first layer is high, we expect that the details of the interactions between particles of the first layer are not relevant, except for preventing the penetration of light particles of the second layer into interstitial regions, which may occur when the system is submitted to vibrations.

The microscopic parameters have been chosen as close as possible to the experimental system. The time step was $\Delta t = 10^{-5}s$, which means that the mean duration of a

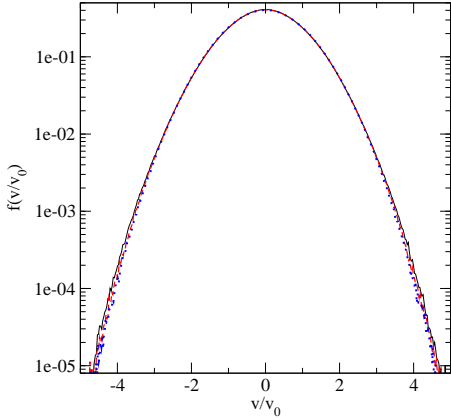


Fig. 2: Renormalized velocity distributions of the light particles for different values of $e_n = 0.5, 0.6, 0.7$ at $\Gamma = 2$ and $c = 0.2$, corresponding respectively to full (black), dashed (red), and dotted (blue) curves. The magenta dashed curve is a Gaussian fit. The renormalizing factor is the root mean squared velocity $v_0 = \sqrt{\langle v^2 \rangle}$

collision is $t_n = 10^{-3}s$. By choosing the normal coefficient e_{n_i} for the different types of collisions, our normal force is then well defined. The mass of the light particles is $M = 22.9mg$, and the mass of the heavy spheres is taken as one half of the mass of the real dimers, namely $m = 92.5mg$. The diameters of light and heavy particles are the same and equal to $3mm$, as in the experiment. The force model described above and the experimental setup lead us to select 5 values of e_{n_i} corresponding to the different types of collision i in the system. We ran simulations for various values of e_{n_i} from 0.4 to 0.8 (see Fig. 2). For these values the deviations of the velocity distributions from Gaussian are weak, but the granular temperature, defined as $T_g = \frac{1}{2}M\langle v^2 \rangle$ (where v is velocity in the xy plane) varies by a factor 3.

The best agreement of the observed T_g with a deviation compatible with experiments is obtained for $e_n = 0.5$ for the particles of the first layer, and we chose $e_n = 0.7$ for the other types of collisions. The value $e_n = 0.5$ for the collisions within the first layer corresponds to strongly dissipative collisions, but the first layer of our system is composed of monomers instead of the dimers used in the experiment. We assume that the dissipation occurring in a layer of composite dimers is much more significant than in a layer of simple spheres. The planar temperature T_g decreases with increasing frequency and with increasing coverage, as observed experimentally. This result is related to the decrease of the amplitude of the excitation in the first case, the light spheres being more likely to sit on the lattice of the first layer, and to the increase of number of collisions in the second case.

Simulations were performed by increasing the coverage

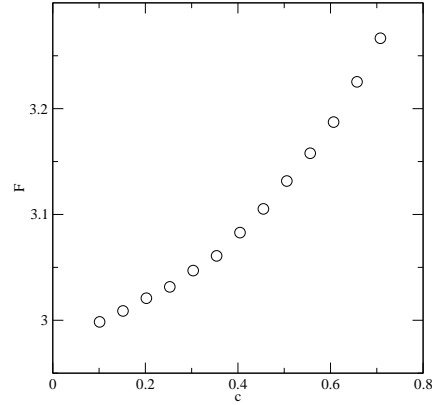


Fig. 3: Kurtosis of the light particles velocity distribution as a function of the coverage of the top layer, other parameters being constant, $\Gamma = 2$, $f = 50Hz$. The Gaussian character remains accurate for moderate densities.

of the top layer, namely increasing the number of the light particles, all others parameters being unchanged ($\Gamma = 2$, e_n , m and M). Figure 3 shows the increase of the kurtosis with the top layer coverage. As expected, at high coverages, the deviations from Gaussian become significant. The remainder of our study is restricted to coverages $c \leq 0.4$.

It is worth noting that with the physical parameters, ($\Gamma = 2$, $c \leq 0.4$), the first layer kurtosis of the heavy particles is always significantly higher than that of the light particles, i.e. $|F - 3| \geq 1$, whereas the values of the second layer are very close to Gaussian ones, with $|F - 3| \leq 0.1$. Finally, we have also studied the influence of the mass ratio of the two species on the velocity distributions: the kurtosis F associated with the light particle velocity distribution is plotted as a function of the mass ratio M/m (see Fig.4) for two values of the coverage $c = 0.2, 0.4$ and exhibits small variations with the mass ratio.

In summary, our simulation model captures the main characteristics of the velocity distribution for different values of the coefficient of restitution, as well as for different densities of the light particles. In order to determine the origin of the Gaussian profile of the horizontal velocity distribution, we monitored trajectories of the light particles as well as the type of collisions occurring during a finite duration (see Fig. 5). Before colliding with another particle of the top layer, a light particle undergoes one or more collisions with the heavy particles, which randomizes the horizontal velocities, and finally leads to a quasi-Gaussian distribution. When the coverage of the top layer increases, the collisions between light particles become more frequent than the collisions between the light and heavy particles, and the velocity distribution progressively loses its Gaussian character. This is illustrated in Fig. 3 which shows

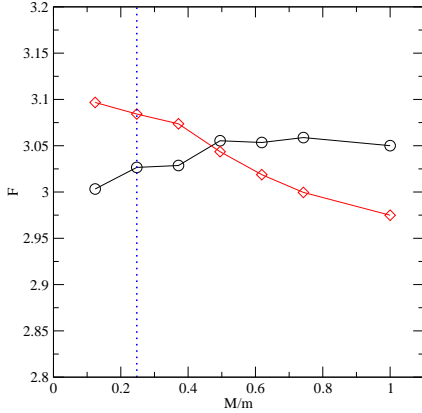


Fig. 4: Kurtosis as a function of the ratio of the light particles mass to the heavy particles mass. Black circles and red diamonds correspond to $c = 0.2, 0.4$ respectively. The dotted vertical line corresponds to the experimental mass ratio.

the variation of the kurtosis of the light particles velocity distribution with the coverage density.

When a collision between particles of different species occurs, the post-collisional velocity of the light particle is randomized due to both the roughness of the first layer and the thermal velocity of the heavy particles. In order to quantify the respective role of each contribution, we performed additional simulations where the heavy particles are glued to the vibrating plate, all remaining parameters being unchanged: in this case, the kurtosis is about 2.9 for a coverage density $c = 0.2$. Whereas the surface roughness of the first layer randomizes the direction of the post-collisional velocity of the light particles, this sole mechanism is not sufficient to lead to a very good Gaussian velocity profile. When the heavy particles are allowed to move, the magnitude of the light particle velocity is modified randomly during a collision. Combining these two mechanisms eventually allows one to obtain a very accurate Gaussian profile.

To verify the homogeneity of the top layer, we have also monitored the longitudinal and transverse velocity correlation functions [3], $C_{\parallel,\perp}(r) = \sum_{i \neq j} v_i^{\parallel,\perp} v_j^{\parallel,\perp} / N_r$. Our results are very similar to those obtained on the experimental setup [16], which indicate the absence of spatial correlations for the velocities of the light particles and the presence of molecular chaos. In fact, a very high packing in the bottom layer is a key ingredient for insuring homogeneity of the top layer: in a recent paper, Combs et al [17] have shown that if the packing fraction of the first layer is decreased, holes appear which rapidly corrupt the Gaussian character of the velocity distribution. Indeed, light particles become trapped and the system loses homogeneity. In the experimental setup, the packing fraction of the

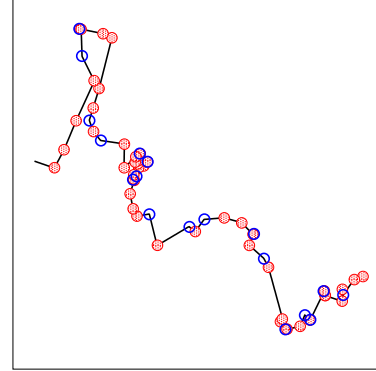


Fig. 5: Trajectory of a particle of the top layer: collisions with bottom particles and other top particles are displayed in red and blue respectively. Blue collisions are on average separated by several red ones. This randomizing process explains the nearly Gaussian character of the top layer velocity distribution.

first layer is high, which prevents the appearance of defects in this first layer.

We have seen that the system is homogeneous, and the non-Gaussian character of the velocity distribution results from the short-time velocity correlations. It is possible to measure the importance of these correlations by considering the first-collision velocity distribution (see Ref [18] for details):

$$P(z) = \langle \delta(z - \mathbf{v} \cdot \mathbf{v}^*) \rangle \quad (4)$$

where \mathbf{v} and \mathbf{v}^* are the velocities of a particle before and after a collision. This quantity is different from the velocity correlation function as it depends on events and not on time. It can be calculated analytically in a few ideal cases such as a granular gas undergoing inelastic collisions, and with the assumptions of a Gaussian velocity distribution and molecular chaos: $P(z)$ has an universal feature in the sense that, for $z < 0$, $P(z)$ is an exponential in any dimension whose analytical expression is given as a function of physical parameters, i.e.,

$$P(z) = P(0) e^{\frac{2}{1+\epsilon_n^2} \sqrt{2(1+\epsilon_n^2)+1-\epsilon_n} \frac{Mz}{T}}, \quad (5)$$

This distribution is a probe for two quantities: (i) it is strongly dependent on the velocity distribution itself and in the case studied here we know the velocity distribution is a Gaussian; (ii) it reveals to what extent precollisional and post-collisional velocities are correlated through the collision process. By sampling separately the two types of collisions undergone by the light particles, we can evaluate and compare their characteristics. Fig.6 displays the two distributions $P_{lh}(z)$ and $P_{ll}(z)$ corresponding to the horizontal velocities. The subscripts lh and ll denote the

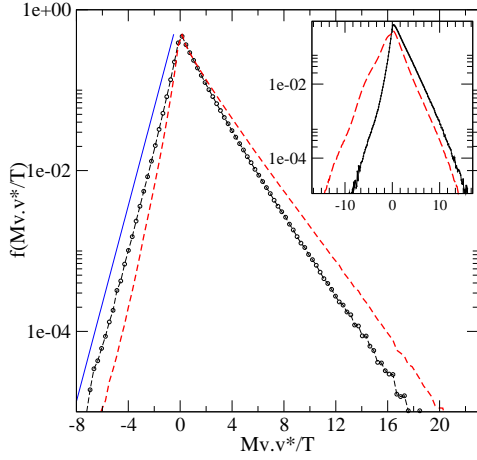


Fig. 6: First-collision horizontal velocity distributions: The dotted (black) and dashed (red) curves correspond respectively to collisions between light particles and between heavy and light particles. The inset displays the first-collision three-dimensional velocity distributions. The solid (blue) curve corresponds to the exponential decay given by Eq.(5) (shifted to the left for clarity).

collisions between heavy and light particles and those between light particles, respectively. $P_{lh}(z)$ would be a simple exponential law if the light particles were reflected by a wall but due to the randomizing effect of the bottom layer, it is very similar to $P_l(z)$. This clearly indicates the similarity of the collision processes within the light beads population and between light and heavy beads: in the horizontal plane, the bottom layer behaves as a nearly Gaussian bath in contact with the light particles population, whereas the heavy particles velocity distribution is far from being Gaussian. The theoretical result, Eq.5, is also shown for $z < 0$, showing an excellent agreement with the simulation results. For completeness, we have also plotted in the inset of Fig.6 the distributions of the three dimensional velocities. For instance, collisions between heavy and light particles are investigated in the decay of $P_{lh}(z)$: note that for $z < 0$, $P_{lh}(z)$ is then far from an exponential, which is closely related to the existence of strongly non-Gaussian velocity distribution in the vertical direction.

In summary, our simple simulation model is in very good agreement with the experimental results of Baxter and Olafsen [14]. Though simple, the model is robust and efficient for the simulation of different vibrated granular systems. We have obtained strong evidence that several ingredients are necessary in order to obtain quasi-Gaussian horizontal velocity distribution for the particles of the top layer, including a rough surface that randomizes the direction of the velocity of the light particle during a collision

with the bottom layer. A more complete randomization is achieved if the amplitude of the velocities of the light particles are changed “randomly” during inter-species collisions: this occurs if the heavy particles are moving. The simulation shows that these features are robust for a large range of microscopic parameters (coefficient of restitution, mass ratio, coverage of the top layer). We encourage an extensive experimental exploration of this setup, for example by substituting anisotropic particles for the top layer spherical particles we used.

We would like to thank G.W.Baxter and J.S.Olafsen for fruitful discussions and for sharing with us their experimental data as well as J. Talbot and R. Hawkins for insightful suggestions.

REFERENCES

- [1] ARANSON I. S. and TSIMRING L. S., *Rev. Mod. Phys.* , **78** (2006) 641.
- [2] MELO F., UMBANHOWAR P. B. and SWINNEY H. L., *Phys. Rev. Lett.* , **75** (1995) 3838.
- [3] PREVOST A., MELBY P., EGOLF D. A. and URBACH J. S., *Phys. Rev. E* , **70** (2004) 050301.
- [4] OLAFSEN J. S. and URBACH J. S., *Phys. Rev. Lett.* , **81** (1998) 4369.
- [5] OLAFSEN J. S. and URBACH J. S., *Phys. Rev. Lett.* , **95** (2005) 098002.
- [6] DAUCHOT O., MARTY G. and BIROLI G., *Phys. Rev. Lett.* , **95** (2005) 265701.
- [7] REIS P. M., INGALE R. A. and SHATTUCK M. D., *Phys. Rev. Lett.* , **98** (2007) 188301.
- [8] VAN NOIJ T. P. C. and ERNST M. H., *Granular Matter* , **1** (1998) 57.
- [9] MONTANERO J. M. and SANTOS A., *Granular Matter* , **2** (2000) 53.
- [10] GARZÓ V. and DUFTY J., *Phys. Rev. E* , **60** (1999) 5706.
- [11] MARTIN P. A. and PIASECKI J., *Europhys. Lett.* , **46** (1999) 613.
- [12] PREVOST A., EGOLF D. A. and URBACH J. S., *Phys. Rev. Lett.* , **89** (2002) 084301.
- [13] REIS P. M., INGALE R. A. and SHATTUCK M. D., *Phys. Rev. E* , **75** (2007) 051311.
- [14] BAXTER G. W. and OLAFSEN J. S., *Nature* , **425** (2003) 680.
- [15] CUNDALL P. and STRACK O., *Geotechnique* , **29** (1979) 47.
- [16] BAXTER G. W. and OLAFSEN J. S., *Phys. Rev. Lett.* , **99** (2007) 028001.
- [17] COMBS K., OLAFSEN J. S., BURDEAU A. and VIOT P., *Phys. Rev. E* , **78** (2008) 042301.
- [18] BURDEAU A. and VIOT P., *Phys. Rev. E* , **78** (2008) 041305.